Graphene gas osmometers

Dolleman, Robin; Cartamil Bueno, Santiago; van der Zant, Herre; Steeneken, Peter

DOI
10.1088/2053-1583/4/1/011002

Publication date
2016

Document Version
Accepted author manuscript

Published in
2D Materials

Graphene Gas Osmometers

Robin J. Dolleman, Santiago J. Cartamil-Bueno, Herre S. J. van der Zant and Peter G. Steeneken

Kavli Institute of Nanoscience, Delft University of Technology, Lorentzweg 1, 2628CJ, Delft, The Netherlands

E-mail: R.J.Dolleman@tudelft.nl

Abstract. We show that graphene membranes that separate two gases at identical pressure are deflected by osmotic pressure. The osmotic pressure is a consequence of differences in gas permeation rates into a few-layer graphene enclosed cavity. The deflection of the membrane is detected by measuring the tension-induced resonance frequency with an interferometric technique. Using a calibration measurement of the relation between resonance frequency and pressure, the time dependent osmotic pressure on the graphene is extracted. The time-dependent osmotic pressure for different combinations of gases shows large differences that can be accounted for by a model based on the different gas permeation rates. In this way, a graphene-membrane based gas osmometer with a responsivity of $\sim$60 kHz/mbar and nanoscale dimensions is demonstrated.

Keywords: Graphene, pressure sensor, gas sensor, osmosis, osmometer, selective permeation

Submitted to: *2D Mater.*

1. Introduction

Graphene, a single layer of sp^2-bonded carbon atoms [1], is impermeable to gases [2]. However, when pristine graphene is suspended over cavities in silicon dioxide, non-zero permeation rates between the cavity and the environment have been measured [2]. The permeation rate was found to depend on the type of gas even in pristine samples [3] and graphene enclosed cavities can therefore be selectively-permeable. The leakage between the cavity and its environment can be attributed to slow permeation through the silicon dioxide layer [2, 4] or along the graphene-oxide interface. In addition, selectivity has also been measured in thinly layered graphene membranes [5].

When a selectively-permeable membrane separates different gases, osmotic gas flow causes a pressure difference across the membrane which is defined as the osmotic pressure [6]. The high Young's modulus [7] and low bending rigidity of graphene cause a large pressure-induced frequency shift and deflection, which is beneficial for several types of pressure sensors[8, 9, 10]. In this work we combine the selective leak rates that graphene-sealed cavities can exhibit with the excellent responsivity that suspended graphene membranes show when subjected to a pressure difference. We use graphene enclosed cavities which are selectively permeable to demonstrate osmotic pressure sensing for several combinations of gases, creating a nanoscale osmometer. Due to osmosis between the cavity and environment, it is observed that a pressure difference builds up over the membrane, even though the pressure on both sides is equal at the start of the experiment. This shows that these systems respond to changes in gas composition in the environment.

We start this paper by explaining the fabrication used to seal cavities with graphene, followed by a brief description of the measurement setup and the calibration procedure (Section 2). Section 3 explains the experimental protocol that was used to measure the time-dependent osmotic pressure. The results obtained from this procedure are presented in Section 4, followed by a discussion of the results (Section 5). The main findings of the work are summarized in the conclusion (Section 6).

2. Fabrication and calibration of osmometers

Graphene membranes are suspended over cavities etched in thermally grown silicon dioxide. A schematic device cross-section is shown in Fig. 1a. A few-layer graphene flake with varying thickness is exfoliated from natural graphite. The flake is transferred by a deterministic dry-transfer method [11] to enclose cavities with a diameter of 3 μm (Fig. 1b–e). It is found that such a device creates a selectively permeable system, without any further processing necessary.

The pressure difference accross the membrane can be determined using the membrane's resonance frequency [2, 3, 9], measured by the interferometric setup shown in Fig. 2a [12, 13]. A modulated blue laser provides opto-thermal actuation, while a red laser is used for interferometric readout of the deflection. A vector network analyzer (VNA) probes the mechanical frequency response of the membrane (Fig. 2b). The sample is mounted in a vacuum chamber with optical access and a dual valve pressure controller is used to keep the pressure in the chamber (p_{ext}) constant throughout the experiment. A line to the vacuum pump is connected to the chamber with a flush valve. The gas in the chamber is changed by switching the gas supply line and opening the flush valve. A needle valve restricts the flow to minimize pressure drops between the controller and the chamber. This prevents membrane deflections

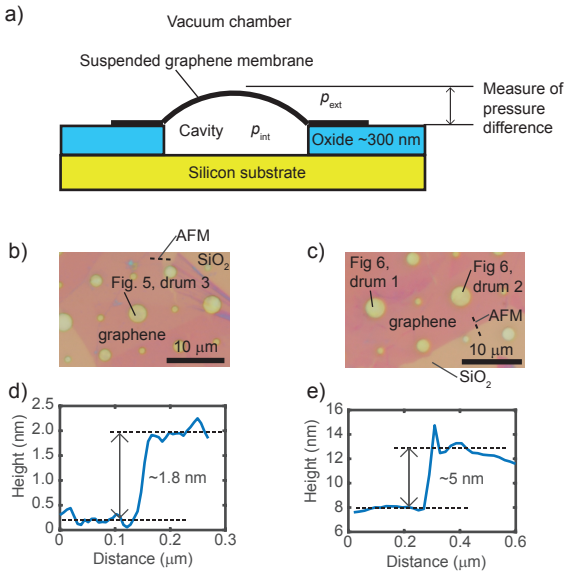

Figure 1. a) Schematics of a graphene-based osmometer. b) Optical image of the graphene resonators presented in this study in Fig. 5. c) Optical image of the graphene resonators presented in Fig. 6. d) Atomic force microscopy (AFM) trace corresponding to Fig. 1b, showing that the graphene resonator has a thickness of about 1.8 nm. e) AFM trace corresponding to Fig. 1c; these drums have a thickness of approximately 5 nm.

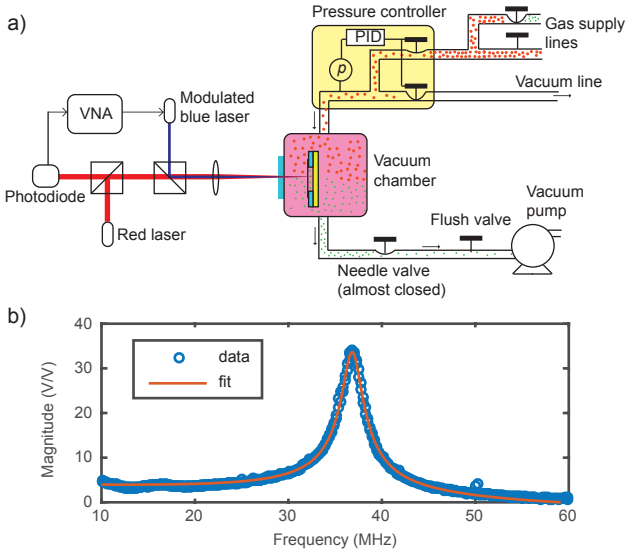

Figure 2. a) Laser interferometer setup (left hand side of the figure) used to detect the resonance frequency and the vacuum chamber with the most important components for flushing the system at constant pressure (right hand side of the figure). b) Example of the measured frequency response, a harmonic oscillator response is fitted which gives a resonance frequency of 36.9 MHz.

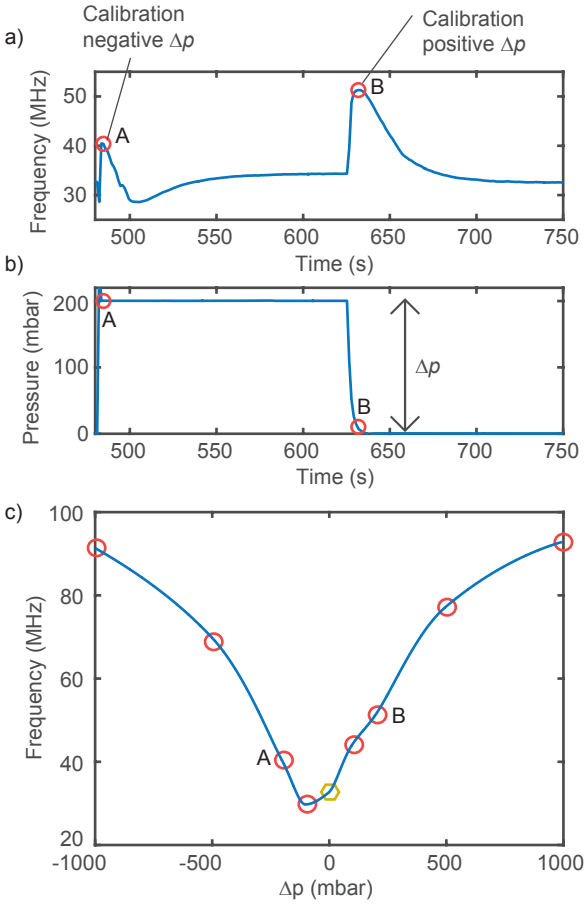

Figure 3. Calibration method to extract the relation between pressure difference and frequency. This figure shows the calibration point for −200 mbar (point A) and +200 mbar (point B) for drum 3. a) Resonance frequency versus time when the external pressure is varied as shown in figure b). c) The calibration curve for drum 3 resulting from the calibration procedure; the hexagon represents the calibration point of the relaxed membrane at a pressure difference of zero and $p_{\text{ext}} = 0$.

due to changes in p_{ext}.

Previous methods to extract the pressure difference from the resonance frequency of the membrane rely on the knowledge of the mechanical properties as mass and Young's modulus and the application of equations governing the membrane behavior [2]. To improve the accuracy of determining the pressure difference over the membrane, we employ a calibration procedure (Fig. 3) from which the relation between pressure difference and resonance frequency is directly determined. The procedure works as follows; first, the membrane is kept in $p_{\text{ext}} = 0$ until the pressure difference is relaxed, which gives the first calibration point (yellow hexagon in Fig. 3c). By increasing the pressure in the chamber rapidly, the membrane will deflect downwards and therefore the pressure difference becomes negative. The immediate change in resonance frequency gives a calibration point at negative pressure (Fig. 3, point A).

Due to the gas leakage, the pressure over the membrane will equilibrate, the frequency is measured at this point to quantify the squeeze-film effect (see Supplementary information). After this, the chamber is rapidly evacuated to $p_{\text{ext}} = 0$. Since the membrane will deflect upwards in that case, a calibration point for positive pressure difference is obtained (Fig. 3, point B). By repeating this procedure for different pressures, the relation between frequency and pressure difference is obtained as shown in Fig. 3c. Using this relation the time-dependent osmotic pressure can be determined in the experiments, without having to rely on knowledge of the mechanical properties of the graphene membrane itself.

It is important to note that from Fig. 3c, it is observed that the minimum in frequency does not correspond to a pressure difference of zero, but is shifted towards negative pressure differences and is around -100 mbar in this case. This is not in agreement with conventional theory which predicts a symmetric response around $\Delta p = 0$. The cause of this effect is unknown, however we take advantage of this effect since it allows us to distinguish between positive and negative pressure differences as shown in section 4. From the calibration curve, it is further concluded that this graphene-based osmometer has an average responsivity of approximately 60 kHz/mbar over the entire pressure range.

3. Experimental procedure

In the experiment, the gas outside the cavity is changed, while the pressure outside the cavity p_{ext} is kept constant. Deflections of the membrane due to external pressure changes are avoided and changes in the pressure difference $\Delta p = p_{\text{int}} - p_{\text{ext}}$ across the membrane should be attributed to changes in the internal pressure p_{int}.

Figure 4a shows the measurement procedure for studying the time dependent osmotic pressure across the membrane. The sample is kept for a long time (at least 1.5 hours) at a constant pressure in gas 1 (red), such that the internal and external pressure equalize $p_{\text{ext}} = p_{\text{int}}$ (Fig. 4a1). The external gas 1 is replaced by gas 2 (green molecules) while keeping the pressure p_{ext} constant (Fig. 4a2,3). This replacement is done rapidly to ensure that gas 1 remains present in the cavity at the same partial pressure as gas 2 in the vacuum chamber ($p_{1,\text{int}} = p_{2,\text{ext}}$). If the leak rate of gas 2 is higher than that of gas 1, gas 2 has a higher flux into the cavity than gas 1 flows out of it. Since the pressure inside the cavity is the sum of the partial pressures of gas 1 and 2, a positive pressure difference Δp arises that is the osmotic pressure (Fig. 4a4). Subsequently, gas 1 will leak out of the cavity at a slower rate (Fig. 4a5) until gas 1 fully disappears and the pressure difference returns to zero $\Delta p \approx 0$ (Fig. 4a6).

In a subsequent measurement gas 2 can be replaced by gas 1 in a similar manner which leads to the sequence shown in Fig. 4d. The main difference is that in this case a negative pressure difference Δp arises. Since the gas leakage has an exponential time dependence (see Supplementary Information) the pressure difference versus time $\Delta p(t)$ can be expressed by the partial pressure differences (Δp_1 and Δp_2) for each gas as a function of time: $\Delta p_1 = p_0 \mathrm{e}^{-t/\tau_1}$ and $\Delta p_2 = -p_0 \mathrm{e}^{-t/\tau_2}$. Combining these equations gives for the total pressure difference:

$$\Delta p(t) = \Delta p_1 + \Delta p_2 = p_0(\mathrm{e}^{-t/\tau_1} - \mathrm{e}^{-t/\tau_2}), \tag{1}$$

where p_0 is the constant pressure in the environment, $\tau_{1,2}$ are the leak-time constants inversely proportional to the permeability of gas 1 and gas 2, respectively. The

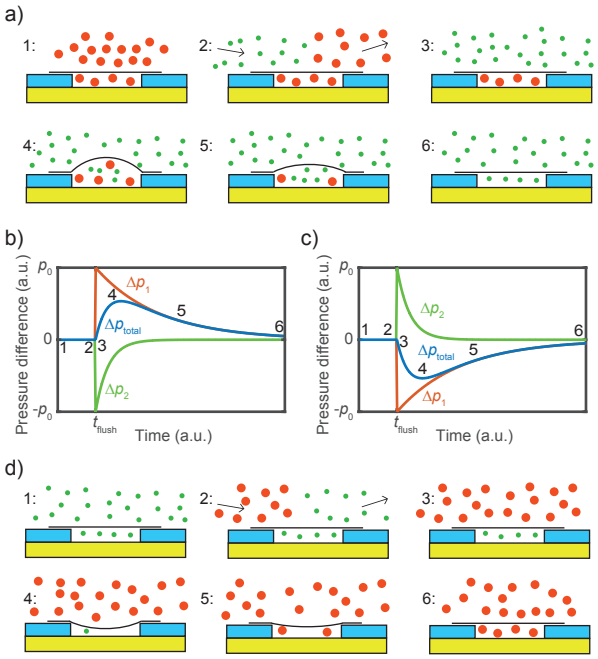

Figure 4. a) Measurement sequence when replacing gas 1 (red) with a large leak time constant τ_1 by gas 2 (green) with a short leak time constant τ_2. b) Time dependent partial pressures differences Δp_{part} of both gases and the total osmotic pressure Δp as described by eq. (1) for the measurement sequences depicted in Fig. 4a. c) Partial pressures and total osmotic pressure for the sequence in Fig. 4d. d) Measurement sequence when replacing gas 2 with a short leak time constant τ_2 by gas 1 (red) with a long leak time constant τ_1.

expected time dependence of the osmotic pressure Δp between two gases 1 and 2 with leak rates τ_2 and τ_1 as described by Eq. (1) is depicted in Fig. 4b,c.

4. Results

Figure 5 shows the results of an experiment where nitrogen gas was replaced with argon gas and vice versa, at a constant chamber pressure of $p_{\text{ext}} = 1000$ mbar. The resonance frequency is found by fitting the data to the frequency response function (Fig. 2b), which in turn yields the time-dependent resonance frequency. To extract the osmotic pressure from the experiment, we use the frequency-pressure difference relation shown in Fig. 3c.

Figure 5a,c show the intensity plots of the frequency response function as function of time. White points indicate the resonance frequencies determined by the fits. The strong difference between the two curves is a consequence of the shifted calibration curve, which allows us to distinguish between positive and negative osmotic pressure. From Fig. 5a we can therefore conclude that argon was permeating into the cavity faster than nitrogen could escape, creating a positive pressure difference. In Fig. 5c, the frequency passes through a minimum twice; a clear indication that a negative pressure difference has formed over the membrane. In this case, argon was escaping the cavity faster than nitrogen could enter. From the time dependent resonance frequency

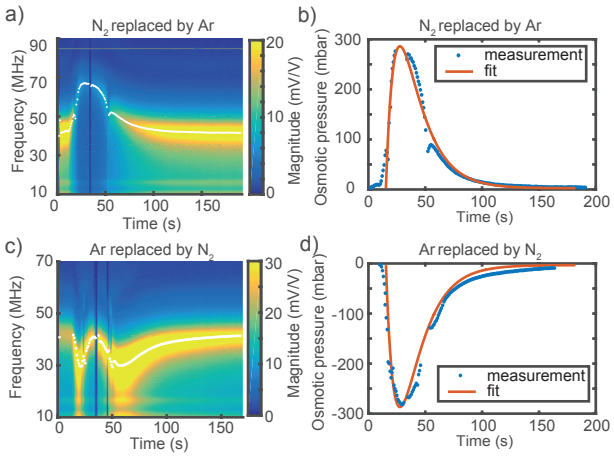

Figure 5. Measurement of the osmotic pressure between argon and nitrogen for drum 3 (Fig. 1b). a) Intensity plot of the frequency response function when nitrogen is replaced by argon in the chamber. White points show the extracted resonance frequency obtained from the fits. b) Osmotic pressure extracted from the experiment in Fig. 5a, fitted by a time-shifted version of eq. (1). c) Intensity plot of the reverse experiment, where argon gas was replaced by nitrogen. d) Extracted osmotic pressure from the experiment in Fig. 5c. The fit from Fig. 5b is plotted with opposite sign.

and the calibration curve in Fig. 3c, the time dependent osmotic pressure can be extracted as shown in Fig. 5b,d. Equation 1 (adapted to include a time shift between the start of the measurement and the gas being replaced) is fitted against the data in Fig. 5b to extract the leak time-constants of the gases [14]: $\tau_{N_2} = 19$ s and $\tau_{Ar} = 8$ s. The osmotic pressure as a function of time from this fit is plotted in Fig. 5d in good correspondence to the measurement result of the reversed experiment. This agreement between both experiments demonstrates that the osmotic pressure reverses sign when interchanging the gases in the experiment.

Figure 6a shows the experimental osmotic pressure versus time for different gas combinations, extracted using the same method as in Fig. 5 but on a different drum. Experiments were carried out with helium, argon, carbon dioxide and nitrogen gas. Equation 1 is fitted to all the 6 osmotic pressure curves to extract the leak time constants as shown in Fig. 6b. A factor of 10 difference is observed in the leak time constant of helium compared to that of nitrogen gas. Also, the time constant of nitrogen is higher in these samples than the thinner sample shown in Fig. 5. Besides thickness, the presence of crystal defects and wrinkles might be reponsible for the observed leak rate differences.

5. Discussion

It is important to note that the presented experiments cannot determine the exact leakage path of the gas molecules into the graphene cavity, although the results do allow to exclude some possible causes. If pores are present that are much larger than the molecular size, Graham's law for effusion predicts leakage rates to be proportional to the square root of the molecular mass ($\tau_1/\tau_2 \propto \sqrt{M_1/M_2}$). However, it is observed that carbon dioxide and helium have almost the same leak rate, despite their large

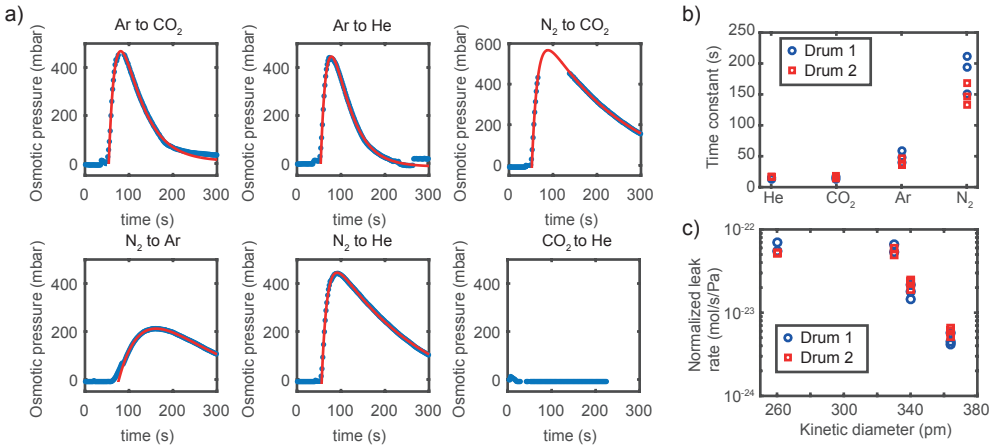

Figure 6. a) Measurement sequences as in Fig. 4a for 6 different gas combinations on a 5 nm thick drum (Drum 1) measured at 500 mbar. b Leak time constants τ extracted for 4 different gases using the fits in Fig. 6a using two different 5 nm thick drums. Drum 2 is measured at 1000 mbar. An optical image of both drums is shown in Fig. 1c. c) Normalized leak rates calculated from the leak time constants in Fig. 6b.

difference in molecular mass. On the other hand, carbon dioxide has a larger mass than nitrogen, but a lower leak rate, again inconsistent with Graham's law for effusion. From this, we conclude that in this study the leakage is not dominated by effusion through pores slightly larger than or comparable to the molecular size of the gases. For example, permeation across pores much larger than the gas molecular dimension but smaller than the gas mean free path has been investigated by Celebi et al. [15], who found that Graham's law does hold true in that case.

Looking at the leak rates for the different gases in Fig. 6b, it is found that they follow the order of the kinetic diameters d of the gases: ($d_{\mathrm{He}} = 260$ pm, $d_{\mathrm{CO_2}} = 330$ pm, $d_{\mathrm{Ar}} = 340$ pm, $d_{\mathrm{N_2}} = 364$ pm). Thus, gases with a kinetic diameter larger than ~330 pm have a lower leak rate than gases with a kinetic diameter smaller than ~330 pm as shown in Fig. 6c. This kind of selectivity in leak rates is similar to the one observed by Koenig et. al. [3] in pristine graphene, although the leak rates observed here are higher. Other research [5] suggests transport could take place between the layers, also resulting in selective gas transport.

If the gas selectivity of the graphene enclosed cavities can be understood and engineered to a larger degree, for example by creating pores of controlled size [3, 16, 17, 18, 19], multiple semi-permeable membranes can be used for gas analysis. This can be achieved by filling these systems with a known gas and subsequently monitoring their time dependent osmotic pressure while exposing them to an unknown gas mixture.

In this work we show results of graphene drums fabricated from natural graphite. These samples showed relatively high lake rates, which allowed repeating the experiment with different gases in a reasonable time span of a few hours. However, in the Supplementary information we show that we can also measure osmosis between cavities sealed by 31 layers of graphene fabricated from KISH-graphite and in cavities sealed by single-layer graphene grown by chemical vapour deposition. These samples

also show selective leakage without any processing necessary, demonstrating that our method can be widely applied.

6. Conclusion

We have demonstrated osmotic pressure sensing with graphene enclosed cavities. The osmotic pressure is a consequence of differences in the molecular leakage rate, which reduces with increasing kinetic diameter, resulting in a spontaneous flux of gas against the pressure gradient. Due to the high flexibility and Young's modulus of graphene, the responsivity of the graphene osmometer is as high as 60 kHz/mbar. We show that these systems are thus able to detect changes of gas composition in its environment, even when the pressure in this environment is kept constant.

Acknowledgments

We thank Dejan Davidovikj, Yaroslav Blanter and Farbod Alijani for discussions and Applied Nanolayers B.V. for supplying the single-layer graphene grown by chemical vapour deposition. The authors further thank the Dutch Technology Foundation (STW), which is part of the Netherlands Organisation for Scientific Research (NWO), and which is partly funded by the Ministry of Economic Affairs, for financially supporting this work. The research leading to these results has also received funding from the European Union Seventh Framework Programme under grant agreement number 604391 Graphene Flagship.

References

[1] Andre K Geim and Konstantin S Novoselov. The rise of graphene. *Nature materials*, 6(3):183–191, 2007.

[2] J Scott Bunch, Scott S Verbridge, Jonathan S Alden, Arend M Van Der Zande, Jeevak M Parpia, Harold G Craighead, and Paul L McEuen. Impermeable atomic membranes from graphene sheets. *Nano letters*, 8(8):2458–2462, 2008.

[3] Steven P Koenig, Luda Wang, John Pellegrino, and J Scott Bunch. Selective molecular sieving through porous graphene. *Nature nanotechnology*, 7(11):728–732, 2012.

[4] Steven P Koenig, Narasimha G Boddeti, Martin L Dunn, and J Scott Bunch. Ultrastrong adhesion of graphene membranes. *Nature nanotechnology*, 6(9):543–546, 2011.

[5] Hyo Won Kim, Hee Wook Yoon, Seon-Mi Yoon, Byung Min Yoo, Byung Kook Ahn, Young Hoon Cho, Hye Jin Shin, Hoichang Yang, Ungyu Paik, Soongeun Kwon, et al. Selective gas transport through few-layered graphene and graphene oxide membranes. *Science*, 342(6154):91–95, 2013.

[6] Eric M Kramer and David R Myers. Five popular misconceptions about osmosis. *American Journal of Physics*, 80(8):694–699, 2012.

[7] Changgu Lee, Xiaoding Wei, Jeffrey W Kysar, and James Hone. Measurement of the elastic properties and intrinsic strength of monolayer graphene. *science*, 321(5887):385–388, 2008.

[8] Shou-En Zhu, Murali Krishna Ghatkesar, Chao Zhang, and GCAM Janssen. Graphene based piezoresistive pressure sensor. *Applied Physics Letters*, 102(16):161904, 2013.

[9] Robin Joey Dolleman, Dejan Davidovikj, Santiago José Cartamil-Bueno, Herre SJ van der Zant, and Peter Gerard Steeneken. Graphene squeeze-film pressure sensors. *Nano letters*, 16(1):568–571, 2016.

[10] AD Smith, Frank Niklaus, A Paussa, Sam Vaziri, Andreas C Fischer, Mikael Sterner, Fredrik Forsberg, Anna Delin, D Esseni, P Palestri, M Ostling, and MC Lemme. Electromechanical piezoresistive sensing in suspended graphene membranes. *Nano letters*, 13(7):3237–3242, 2013.

[11] Andres Castellanos-Gomez, Michele Buscema, Rianda Molenaar, Vibhor Singh, Laurens Janssen, Herre SJ van der Zant, and Gary A Steele. Deterministic transfer of two-dimensional materials by all-dry viscoelastic stamping. *2D Materials*, 1(1):011002, 2014.

[12] Andres Castellanos-Gomez, Ronald van Leeuwen, Michele Buscema, Herre SJ van der Zant, Gary A Steele, and Warner J Venstra. Single-layer mos2 mechanical resonators. *Advanced Materials*, 25(46):6719–6723, 2013.

[13] Dejan Davidovikj, Jesse J Slim, Santiago J Cartamil-Bueno, Herre SJ van der Zant, Peter G Steeneken, and Warner J Venstra. Visualizing the motion of graphene nanodrums. *Nano letters*, 16(4):2768–2773, 2016.

[14] Per Sundqvist. Exponential curve-fitting, without start-guess. retrieved 14 March 2016 from: http://www.mathworks.com/matlabcentral/fileexchange/21959-exponential-fit–without-start-guess.

[15] Kemal Celebi, Jakob Buchheim, Roman M Wyss, Amirhossein Droudian, Patrick Gasser, Ivan Shorubalko, Jeong-Il Kye, Changho Lee, and Hyung Gyu Park. Ultimate permeation across atomically thin porous graphene. *Science*, 344(6181):289–292, 2014.

[16] Ryan C Rollings, Aaron T Kuan, and Jene A Golovchenko. Ion selectivity of graphene nanopores. *Nature communications*, 7, 2016.

[17] Sumedh P Surwade, Sergei N Smirnov, Ivan V Vlassiouk, Raymond R Unocic, Gabriel M Veith, Sheng Dai, and Shannon M Mahurin. Water desalination using nanoporous single-layer graphene. *Nature nanotechnology*, 10(5):459–464, 2015.

[18] Sean C O'Hern, Doojoon Jang, Suman Bose, Juan-Carlos Idrobo, Yi Song, Tahar Laoui, Jing Kong, and Rohit Karnik. Nanofiltration across defect-sealed nanoporous monolayer graphene. *Nano letters*, 15(5):3254–3260, 2015.

[19] Sean C O'Hern, Michael SH Boutilier, Juan-Carlos Idrobo, Yi Song, Jing Kong, Tahar Laoui, Muataz Atieh, and Rohit Karnik. Selective ionic transport through tunable subnanometer pores in single-layer graphene membranes. *Nano letters*, 14(3):1234–1241, 2014.